

Practical issues of twin-field quantum key distribution

Feng-Yu Lu,^{1,2} Zhen-Qiang Yin,^{1,2,*} Rong-Wang,^{1,2} Guan-Jie Fan-Yuan,^{1,2} Shuang Wang,^{1,2} De-Yong He,^{1,2} Wei Chen,^{1,2} Wei Huang,³ Bing-Jie Xu,³ Guang-Can Guo,^{1,2} and Zheng-Fu Han^{1,2}

¹*CAS Key Laboratory of Quantum Information,
CAS Center For Excellence in Quantum Information and Quantum Physics,
University of Science and Technology of China, Hefei 230026, China*

²*State Key Laboratory of Cryptology, P. O. Box 5159, Beijing 100878, China*

³*Science and Technology on Communication Security Laboratory,
Institute of Southwestern Communication, Chengdu, Sichuan 610041, China*

Twin-Field Quantum Key Distribution(TF-QKD) protocol and its variants, such as Phase-Matching QKD(PM-QKD), sending or not QKD(SNS-QKD) and No Phase Post-Selection TF-QKD(NPP-TFQKD), are very promising for long-distance applications. However, there are still some gaps between theory and practice in these protocols. Concretely, a finite-key size analysis is still missing, and the intensity fluctuations are not taken into account. To address the finite-key size effect, we first give the key rate of NPP-TFQKD against collective attack in finite-key size region and then prove it can be against coherent attack. To deal with the intensity fluctuations, we present an analytical formula of 4-intensity decoy state NPP-TFQKD and a practical intensity fluctuation model. Finally, through detailed simulations, we show NPP-TFQKD can still keep its superiority of high key rate and long achievable distance.

arXiv:1901.04264v3 [quant-ph] 16 Apr 2019

* yinzq@ustc.edu.cn

I. INTRODUCTION

Quantum Key Distribution(QKD)[1, 2] is one of the most mature applications among the emerging quantum technologies. It allows two remote users, called Alice and Bob, to share random secret keys even if there is an eavesdropper, Eve[3–5]. Due to the loss of channel, both the key rate and achievable distance of QKD are limited. Although increasing the secret key rate(SKR) and achievable distance are essentially significant for the real applications of QKD, the theorists proved there are some limits on the improvement of SKR[6, 7]. In particular, for the channel of transmittance η , the linear bound [7], i.e. $R \leq -\log_2(1 - \eta)$, gives the precise SKR bound for any point-to-point QKD without quantum repeaters. Surprisingly, a revolutionary protocol called Twin-Field Quantum Key Distribution(TF-QKD)[8] was recently proposed to beat this bound. Inspired by the novel idea of TF-QKD, researchers proposed some variants and completed the corresponding security proofs [9–14]. From the view of experiments, these variants, i.e. Phase-Matching QKD(PM-QKD)[10], sending or not QKD(SNS-QKD)[11] and No Phase Post-Selection TF-QKD(NPP-TFQKD)[12–14], are simpler. Indeed, both the SNS-QKD and NPP-TFQKD have been successfully demonstrated[15–18].

However, there are still some gaps between theory and implementation of TF-QKD. The first problem is the finite-key size effect is still not considered previously. In Refs.[12–14], asymptotic SKR of NPP-TFQKD is proposed, but the SKR in finite-key region is not given. On the other hand, the key-size in a practical implementation is always finite, thus a framework to deal with the finite-key size effect in TF-QKD is indispensable.

Another problem we will discuss is a potential security loophole of TF-QKD and its variants. Although the Refs.[8–14] have proved the TF-QKD and its variants are information-theoretically secure even with untrusted measurement device just like the original measurement-device-independent protocol[19–22], the imperfections of laser source may spoil the security. One of the intractable loopholes of source is the intensity fluctuation[23–25]. In the existing security proofs of NPP-TFQKD, it is assumed that Alice and Bob are able to accurately control the intensity of signal and decoy modes, which is not perfectly satisfied in experiment. In this work, we also propose a countermeasure to tackle the intensity fluctuation of NPP-TFQKD. A key step of our method is proposing the analytical formulas to deal with the 4-intensity decoy states in NPP-TFQKD. In the original NPP-TFQKD[12], one must use linear programming to solve linear equations of decoy states [26–30]. Compared with linear programming, analytical formula has superiorities on some special situations. More importantly, the proposed analytical formulas are particularly convenient to be incorporated to our intensity fluctuation. Another key step of our method is introducing a new intensity fluctuation model in finite-key size regime. The model makes TF-QKD robust to intensity fluctuation.

The rest of this paper is organized as following. Firstly, In Sec.II, we briefly review the flow of NPP-TFQKD protocol. In Sec.III, we analyze the finite-key size effect of NPP-TFQKD, give the SKR formula against coherent attack and evaluate the performance of TF-QKD in finite-key regime. In Sec.IV, the analytical formulas for 4-intensity decoy state method are given. Then we introduce the intensity fluctuation model and its countermeasure. Finally, a completed simulation taken both the finite-key size effect and intensity fluctuation into account is present.

II. PROTOCOL DEFINITION

The setup of NPP-TFQKD[12] protocol is illustrated in Fig.1 and the flow is as following:

State preparation: This step will be repeated by N trials. In each trial, Alice(Bob) chooses code mode or decoy mode with probabilities P_c and $P_d = 1 - P_c$ respectively, sends corresponding quantum state to untrusted Charlie.

When code mode is selected, Alice(Bob) prepares a phase-locked weak coherent pulse(WCP) $|\pm\sqrt{\mu}\rangle_A(|\pm\sqrt{\mu}\rangle_B)$, where the plus or minus of the quantum state depends on the bit value of Alice(Bob)'s random key of this trial.

When decoy mode is selected, Alice(Bob) prepares a phase randomized WCP, whose intensity $\nu_a(\nu_b)$ is randomly chosen from a pre-decided set. Alice(Bob) actually prepares a mixed state since the randomized phase in the decoy mode will never be publicly announced. For instance, the density matrix of Alice's WCP

in decoy mode can be denoted as:

$$\rho_{\nu_a} = \sum_{n=0}^{\infty} e^{-\nu_a} \frac{\nu_a^n}{n!} |n\rangle\langle n|, \quad (1)$$

where $|n\rangle$ is the Fock state.

Measurement: For each trail of the state preparation step, the untrusted Charlie must publicly announce a single click of his single photon detector (SPD) 'SPD-L' or 'SPD-R' or non-click message. Note that Charlie is untrusted, thus he is not necessarily to make the measurement shown in Fig.1.

Sifting: Alice and Bob publicly announce which trails are code mode and which are decoy mode. For the trials they both choose code mode and Charlie announce 'SPD-L' or 'SPD-R' clicked, Alice and Bob will retain this key bit. According to Charlie's measurement result, Bob may decide to flip his key bit or not. After this step, Alice and Bob generate sifted key bit string Z and Z' respectively.

Error correction: Alice sends $\lambda_{EC} = nfH(E_c)$ bits of classical error correction data to Bob. Here $n=|Z|=|Z'|$ is the size of sifted key bits, $H(p) = -p\log_2 p - (1-p)\log_2(1-p)$ is the Shannon entropy, E_c is the error rate of sifted key bits and $f \geq 1$ denotes error correction efficiency. Depending on the error correction data and Z' , Bob obtains an estimated \hat{Z} of Z . Next, by applying universal₂ hash function, Alice sends $\lambda_{EV} = \log_2 \frac{1}{\epsilon_{cor}}$ bits of error verification information to Bob. If the error verification fails, they output an empty string and abort the protocol. Otherwise, they assume the error correction succeeds and $Z = \hat{Z}$.

Parameter estimation and privacy amplification: Alice and Bob accumulate data to estimate gain Q_c of trials that they both choose code mode, gains Q_{xy} of trials they choose decoy mode with intensity x and y respectively. With these parameters and $\lambda_{EC}, \lambda_{EV}$, Alice and Bob perform privacy amplification, say, apply a random universal₂ hash function to Z and \hat{Z} respectively to generate l_{sec} -length secure bit string S and S' respectively. The SKR per pulse is defined as $R = l_{sec}/N$

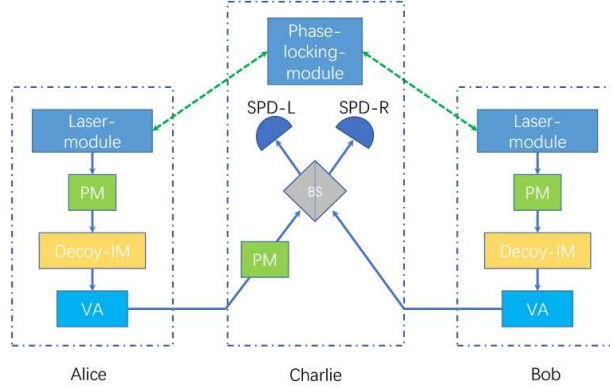


FIG. 1. In Alice and Bob's side, The laser-modules can prepare initial phase locked weak coherent pulses with the help of the phase-locking module belongs to Charlie[16]. The phase-modulators(PM) are apply to encode key bits in code mode and randomize the phase of WCPs in decoy mode. The intensity-modulators(decoy-IM) are set to modulate different intensities to apply decoy state technique. VA denotes variable attenuator. The PM belongs to Charlie can compensate phase drift caused by long-distance fiber. The gray square denotes 50:50 beam splitter and the blue semicircles are single photon detectors(SPDS)

III. FINITE-KEY ANALYSIS OF NPP-TFQKD

Previous works[12–14] of NPP-TFQKD are based on the asymptotic situation. However, since it's impossible for Alice and Bob to send infinite pulses to generate their secure key in reality, the finite-key size effect[31–34] must be taken into account. In this section, we first extend the asymptotic SKR formula of

Ref.[12] to non-asymptotic one against collective attack. Then based on the postselection technique developed in Ref.[31], a formula against coherent attack is present.

A. Security definition and SKR against collective attack

As discussed above, in the end of NPP-TFQKD, Alice and Bob obtain a pair of bit string S and S' respectively. Ideally, the bit strings are secure and applicable to any cryptosystem if two fundamental conditions are met, namely correctness and secrecy. The correctness is, in simple terms, $S = S'$, which is guaranteed by the error verification. The secrecy requires Eve's system E is decoupled from Alice's key S , which is illustrated by $\rho_{SE} = U_S \otimes \rho_E$, where $\rho_{SE} = \sum_s (|s\rangle\langle s| \otimes \rho_E^s)$ denotes the density matrix of Alice and Eve's quantum state, $U_S = \sum_s \frac{1}{|S|} |s\rangle\langle s|$ denotes the uniform mixture of all possible value of S , $\{|s\rangle\}$ denotes the orthonormal basis of Alice's key S and ρ_E^s is Eve's the density matrix of Eve's system conditioned that Alice's key S is in the state $|s\rangle$. Clearly, Alice's key S is completely unknown to Eve in this ideal case.

However, in finite-key size regime, the ideal condition $\rho_{SE} = U_S \otimes \rho_E$ usually can't be perfectly met. In Ref.[35], a composable security criteria is proposed. This criteria introduces secure parameters to describe some small probabilities of the keys S and S' varying from the ideal case. The protocol is ϵ_{cor} -correct if $P(S \neq S') \leq \epsilon_{cor}$, i.e. the probability of $S \neq S'$ is less than ϵ_{cor} . Similarly, the protocol is ϵ_{sec} -secret if $\frac{1}{2} \|\rho_{SE} - U_S \otimes \rho_E\|_1 \leq \epsilon_{sec}$, which means ρ_{SE} is ϵ_{sec} close to the ideal situation $U_S \otimes \rho_E$, where the symbol $\|M\|_1$ denotes trace norm of matrix M . In general, if a protocol is ϵ -secure, $\epsilon_{cor} + \epsilon_{sec} \leq \epsilon$ must hold. To meet this criteria, with the same manner of Ref.[32], the SKR formula of NPP-TFQKD against collective is given by

$$R_{col} = \frac{n}{N} [1 - \bar{I}_{AE}] - \frac{1}{N} \lambda_{EC} - \frac{1}{N} \lambda_{EV} - \frac{2}{N} \log_2 \frac{1}{\epsilon_{PA}} - \frac{7}{N} \sqrt{n \log_2(2/\epsilon_s)}, \quad (2)$$

where $n = P_c^2 Q_c N$ is the size of sifted key bits, \bar{I}_{AE} is the upperbound of Eve's information on the sifted key bit if she launches collective attack, $\lambda_{EV} = \log_2 \frac{2}{\epsilon_{cor}}$ implies that $P(S \neq S') \leq \epsilon_{cor}$, ϵ_{PA} accounts for the probability of failure of privacy amplification, and ϵ_s measures the accuracy of the estimating the smooth min-entropy[32]. As shown in Ref.[12], the estimation of \bar{I}_{AE} against collective attack depends on some experimentally observed parameters including the gains Q_c and Q_{xy} . When the number of trials is finite, the expectations of these gains may vary from the experimentally observed values due to statistical fluctuations. Thus, another secure parameter ϵ_{PE} [34] characterizing the probability that parameter estimation fails must be taken into account. For instance, consider a set of *i.i.d.* random variables $X_1 X_2 \dots X_N (X_i \in \{0, 1\})$, the observed frequency of bit 1 is usually not equal to its expectation $E(X)$, provided N is finite. To solve this problem, we apply large deviation theory, specifically, the Chernoff bound to estimate a confidence interval of X according to the observed value. In NPP-TFQKD, we can apply Chernoff bound[34, 36, 37] to estimate Q_c and Q_{xy} through the observed gains \hat{Q}_c and \hat{Q}_{xy} with a failure probability ϵ_{PE} respectively. For instance, we have that the expectation value of the gain Q_{xy} satisfied $Q_{xy}^- \leq Q_{xy} \leq Q_{xy}^+$ with probability $1 - \epsilon_{PE}$, where

$$\begin{aligned} Q_{xy} &\geq Q_{xy}^- = \hat{Q}_{xy} \left(1 - \frac{f(\epsilon_{PE}^4/16)}{\sqrt{N_{xy} \hat{Q}_{xy}}}\right), \\ Q_{xy} &\leq Q_{xy}^+ = \hat{Q}_{xy} \left(1 + \frac{f(\epsilon_{PE}^4/16)}{\sqrt{N_{xy} \hat{Q}_{xy}}}\right), \end{aligned} \quad (3)$$

, $f(\epsilon) = \sqrt{2 \ln(\epsilon^{-1})}$, and N_{xy} denotes the total number of trials which Alice and Bob select decoy mode with intensity x and y , respectively. As there are totally 11 gains to estimate in NPP-TFQKD [12], the probability of occurring any failure in the estimations of 11 gains is $11\epsilon_{PE}$. Then applying the worst-case fluctuation analysis in the calculation of linear programming[30, 36], we can bound $Y_{nm} (n + m \leq 2)$, where Y_{nm} is the

probability of Charlie announcing a click message conditioned that Alice and Bob send Fock states $|n\rangle$ and $|m\rangle$ respectively. Furthermore, with Eq.(2) in Ref.[12], we obtain \bar{I}_{AE} with the failure probability of $11\epsilon_{PE}$.

Finally, Alice and Bob generate NR_{col} bits secret key against collective attack with ϵ_{col} -security. Obviously, ϵ_{col} is not exceeding the sum of failure probabilities of error verification, privacy amplification, accuracy of smooth min-entropy and parameters estimation, say,

$$\epsilon_{col} \leq \epsilon_{PA} + \epsilon_{cor} + \epsilon_s + 11\epsilon_{PE}. \quad (4)$$

Now we have introduced how to generate ϵ_{col} -security keys against collective attack in NPP-TFQKD with finite-key effect. Next, we discuss how to obtain ϵ_{coh} -security keys against coherent attack.

B. Countermeasure of coherent attack

According to Ref.[31], it is proved that for a QKD protocol, the security against collective attack could be extended to be against coherent attack easily. We introduce the following corollary from the theorem 1 of Ref.[31] to tackle coherent attack in finite-key region.

Corollary. The key rate R_{coh} against coherent attack could be given by

$$R_{coh} = R_{col} - \frac{126\log_2(N+1)}{N}, \quad (5)$$

while the key is ϵ_{coh} -secure and

$$\epsilon_{coh} = \epsilon_{col}(N+1)^{63}. \quad (6)$$

Proof. The proof is based on the theorem 1 of Ref.[31] and very similar proofs can be found in Ref.[31] and the appendix B of Ref.[32]. We denote \mathcal{H}_A , \mathcal{H}_B , and \mathcal{M} are the Hilbert space of Alice's ancilla A , Bob's ancilla B and Charlie's message M respectively. Without compromising the security, Charlie's message M (click or not) can be treated as a quantum state shared by Alice and Bob. The NPP-TFQKD protocol using Eq.2 to generate keys could be viewed as a map \mathcal{E} transforming A , B and M into keys S and S' ($|S| = |S'| = NR_{col}$) respectively. Let \mathcal{S} be a hypothetical map transforming imperfect keys S and S' into perfect ones and define $\mathcal{F} = \mathcal{S} \circ \mathcal{E}$. Recall last subsection, it asserts that $\|((\mathcal{E} - \mathcal{F}) \otimes id)\tau_{\mathcal{H}^N \mathcal{K}^N}\|_1 \leq \epsilon_{col}$ holds when Eq.2 is used to generate keys, where the de Finetti-Hilbert-Schmidt state $\tau_{\mathcal{H}^N \mathcal{K}^N} = \int \sigma_{\mathcal{H}\mathcal{K}}^{\otimes N} \mu(\sigma_{\mathcal{H}\mathcal{K}})$, $\mathcal{H} = \mathcal{H}_A \otimes \mathcal{H}_B \otimes \mathcal{M}$, $\sigma_{\mathcal{H}\mathcal{K}}$ is the pure state shared by Alice, Bob and Eve induced by any collective attack, and $\mu(\sigma_{\mathcal{H}\mathcal{K}})$ is the Haar measure on the pure state $\sigma_{\mathcal{H}\mathcal{K}}$.

Next, we consider Eve may control another ancilla R to obtain the purification $\tau_{\mathcal{H}^N \mathcal{K}^N \mathcal{R}}$ of $\tau_{\mathcal{H}^N \mathcal{K}^N}$. For such a purification, $dim(\mathcal{R})$ is not larger than $(N+1)^{d^2-1}$ [31] where $d = dim(\mathcal{H} \otimes \mathcal{K}) = 8$. Through controlling ancilla R , Eve's min-entropy on sifted key is decreased at most $2(d^2-1)\log_2(N+1)$ bits. To meet the security, Alice and Bob may perform protocol \mathcal{E}' , in which privacy amplification shortens the sifted key into $NR_{col} - 2(d^2-1)\log_2(N+1)$ bits. Then we have $\|((\mathcal{E}' - \mathcal{F}') \otimes id_{\mathcal{K}^N \mathcal{R}})\tau_{\mathcal{H}^N \mathcal{K}^N \mathcal{R}}\|_1 \leq \epsilon_{col}$ still holds, where \mathcal{F}' is a hypothetical map generating perfect keys.

Finally, we apply the theorem 1 of Ref.[31] and obtain

$$\|((\mathcal{E}' - \mathcal{F}') \otimes id_{\mathcal{K}^N \mathcal{R}})\rho_{\mathcal{H}^N \mathcal{K}^N \mathcal{R}}\|_1 \leq \|((\mathcal{E}' - \mathcal{F}') \otimes id_{\mathcal{K}^N \mathcal{R}})\tau_{\mathcal{H}^N \mathcal{K}^N \mathcal{R}}\|_1 \leq \epsilon_{col}(N+1)^{d^2-1}.$$

Since $\rho_{\mathcal{H}^N \mathcal{K}^N \mathcal{R}}$ is any state shared by Alice, Bob and Eve, this inequality clearly shows that the protocol \mathcal{E}' is $\epsilon_{col}(N+1)^{d^2-1}$ -secure for any coherent attack. Substituting $d = 8$, we end the proof. \square

According to the corollary, if Alice and Bob want to generate ϵ_{coh} -secure keys against any attack, they will calculate the parameter ϵ_{col} with Eq.6, and generate keys with the formulae Eqs.5, 2 and 4.

To evaluate the performance of NPP-TFQKD in finite-key region, simulations in fiber channel are performed here. We assume the dark-count rate of SPD is 10^{-10} per trial, the detection efficiency is 14.5% and

optical misalignment is 1.5%. The attenuation of fiber is $0.2\text{dB}/\text{km}$ and the fiber transmittance is $10^{-0.2L/10}$ where L is fiber length. The total secure parameter ϵ_{coh} in Eq.6 is fixed as 10^{-10} . In addition to fixed parameters above, there are some parameters should be optimized to maximize the SKR. There are 10 parameters should be optimized in total. The first set is decoy intensities μ, ν and ω . The second set is probabilities of modes and intensities. P_c denote probabilities of choosing code mode and $P_d^\mu, P_d^\nu, P_d^\omega$ denote probabilities of choosing decoy mode with intensity μ, ν, ω . It worth noting that probabilities of vacuum state is $P_d^o = 1 - P_c - P_d^\mu - P_d^\nu - P_d^\omega$. The number of pulses they both select code mode is NP_c^2 and they select decoy mode with intensity x and y respectively is $NP_d^x P_d^y$. The other set is $\epsilon_{PA}, \epsilon_{cor}, \epsilon_s$ and ϵ_{PE} satisfying Eq.4. Define $\epsilon_{cor} = \epsilon_{col} r_{cor}$, $\epsilon_s = \epsilon_{col} r_s$ and $\epsilon_{PE} = \epsilon_{col}(1 - r_{sec} - r_{cor} - r_s)/11$.

The optimized parameters can be regarded as a vector $\vec{v} = [\mu, \nu, \omega, P_c, P_d^\mu, P_d^\nu, P_d^\omega, r_{sec}, r_{cor}, r_s]$. Noting that the convex form of function $R_{coh} = F(\vec{v})$ [38, 39] is not guaranteed, we choose particle swarm optimization algorithm(PSO) which can optimize the non-smooth function and non-convex function[40] to search the best \vec{v} to maximize the R_{coh} .

The results of the simulations are illustrated in Fig.2 and 3. In Fig.2, we fix the pulses number N to be $10^{12}, 10^{13}, 10^{14}$ and simulate the SKR as a function of distance between Alice and Bob. In Fig.3 the distance is fixed to be $50\text{km}, 100\text{km}$ and 150km , then we simulate the SKR as a function of N . The results show that compared with asymptotic situation, the protocol still works well in non-asymptotic situations and the linear bound is still overcome when $N \geq 10^{12}$.

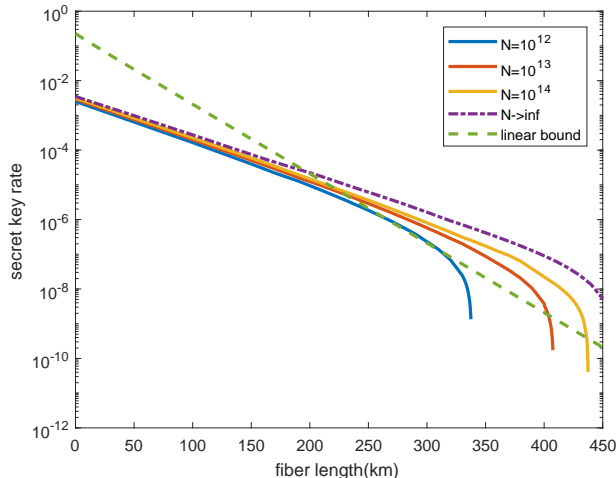


FIG. 2. SKR versus distance between Alice and Bob for three different pulses number ($N = 12$: blue, $N = 13$: red, $N = 14$: yellow). The purple dot-dash line is asymptotic SKR and the green dash line is the linear bound

IV. NPP-TFQKD WITH BOTH LARGE RANDOM INTENSITY FLUCTUATION AND FINITE-KEY SIZE EFFECT

Except for finite-key size effect, a ubiquitous loophole in practical QKD system is intensity fluctuation[23–25]. When applying decoy state technique, accurate intensity values are required to ensure the correct estimation of Y_{nm} [12]. However, it's very difficult to control the intensity of WCP exactly in practical QKD system since noise, time jitter, problem of modulation and other imperfections of devices. It brings potential loopholes and may allow Eve to perform sophisticated attacks. In this section, we discuss the NPP-TFQKD with large random intensity fluctuation in finite-key size regime. The main contribution of this section is that we present a countermeasure of both large random intensity fluctuation and finite-key size effect of NPP-TFQKD. By applying our method, the NPP-TFQKD with large random intensity fluctuation can remain its advantage of breaking the linear bound.

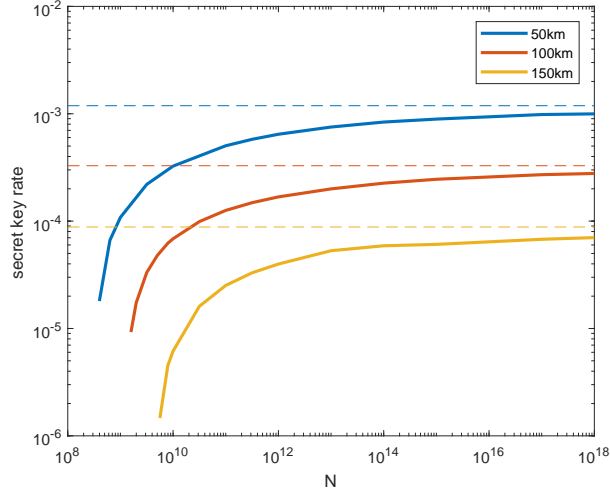


FIG. 3. Secret key rate in logarithmic scale as a function of pulses number N for three different distance between Alice and Bob(50km: blue, 100km: red, 150km: yellow). The solid lines denote non-asymptotic SKR and the dash lines show corresponding asymptotic SKR

A. Analytical formula of 4-intensity decoy state method of NPP-TFQKD

Before proposing the intensity fluctuation model of NPP-TFQKD, we will introduce our analytical formula of 4-intensity decoy state method. In 'Parameter estimation and privacy amplification' step, the n-photon yield can be estimated by linear programming or analytical formula[29, 30]. However, the analytical formula of NPP-TFQKD is not given. In our countermeasure of imperfect WCP source loophole in next section, the analytical formula is needed. To make the NPP-TFQKD more practical, the analytical formula of 4-intensity decoy state method is proposed.

Define $q_{nm} = p_n^\mu p_m^\mu Y_{nm}$ where $p_n^x = e^{-x} \frac{x^n}{n!}$. To estimate the upper bound of I_{AE} , we have to estimate the upper bound of $q_{00}, q_{10}, q_{01}, q_{20}, q_{02}, q_{11}$ and lower bound of $q_{sum} = q_{00} + q_{10} + q_{01} + q_{20} + q_{02} + q_{11}$. The upper and lower bound of Y_{nm} can be estimated by applying linear programming whose constraints are joint of:

$$Q_{xy} = \sum_{n=0}^{\infty} \sum_{m=0}^{\infty} p_n^x p_m^y Y_{nm} \quad (x, y \in \{\mu, \nu, \omega, o\}), \quad (7)$$

where $0 \leq Y_{nm} \leq 1$. Noting that these p_n^x depend on the intensity x , it's obvious that the p_n^x in Eq.(7) are uncertain and the linear programming will be not valid any more if we can't control intensities exactly. Intuitively, we can still get secure bound of key rate if we correctly replace coefficients p_n^x by its upper and lower bound in analytical formula. Thus we present an analytical formula before building the fluctuation model.

We will use superscript '+' and '-' to express, respectively, upper and lower bound of a variable and we denote intensities in decoy mode by μ, ν, ω, o where $\mu > \nu > \omega > o$ and o is the vacuum state. It is worth noting that, the intensity of code mode should be the same as one of μ, ν or ω . To make our formula more clear, we suppose code mode intensity is μ and denote $p_n^\mu, p_n^\nu, p_n^\omega$ by a_n, b_n, c_n .

Here we will demonstrate how to estimate n-photon yield by analytical formulas as follows. The details are showed in Appendix.

Estimation of q_{00} :

$$q_{00} = a_0^2 Q_{oo}.$$

Upper bound of q_{10} and q_{01} :

$$q_{10}^+ = a_0 a_1 \frac{K_2(c_2 a_3 - c_3 a_2) + K_1(b_2 c_3 - b_3 c_2) + K_3(a_2 b_3 - a_3 b_2)}{b_2(a_1 c_3 - c_1 a_3) + b_1(c_2 a_3 - c_3 a_2) + b_3(a_2 c_1 - a_1 c_2)}, \quad (8)$$

where $K_1 = Q_{\mu o} - a_0 Q_{oo}$, $K_2 = Q_{\nu o} - b_0 Q_{oo}$ and $K_3 = Q_{\omega o} - c_0 Q_{oo}$.

Expression of q_{01}^+ is similar, the difference is $K_1 = Q_{o\mu} - a_0 Q_{oo}$, $K_2 = Q_{o\nu} - b_0 Q_{oo}$, $K_3 = Q_{o\omega} - c_0 Q_{oo}$.

Upper bound of q_{20} and q_{02} :

$$q_{20}^+ = a_0 a_2 \frac{H_1 c_1 - L_3 a_1}{a_2 c_1 - a_1 c_2}, \quad (9)$$

where $H_1 = Q_{\mu o} - a_0 Q_{oo}$, $L_3 = Q_{\omega o} - c_0 Q_{oo} - (\sum_{n=3}^{\infty} c_n)$. Formula of q_{02}^+ is similar but $H_1 = Q_{o\mu} - a_0 Q_{oo}$, $L_3 = Q_{o\omega} - c_0 Q_{oo} - (\sum_{n=3}^{\infty} c_n)$.

Upper bound of q_{11} :

$$q_{11}^+ = Q_{\mu\mu} - a_0(Q_{\mu o} + Q_{o\mu}) + a_0^2 Q_{oo}. \quad (10)$$

Lower bound of q_{sum} :

We take two steps to calculate the q_{sum}^+ . Define $q_{sum} = q_{t_1} + q_{t_2}$, where $q_{t_1} = q_{00} + q_{10} + q_{01} + q_{20} + q_{02} + q_{11}$ and $q_{t_2} = q_{11}$.

$$q_{t_1}^- = a_0 [Q_{o\mu} + Q_{\mu o} - 2 \sum_{n=3}^{\infty} a_n] - a_0^2 Q_{oo}, \quad (11)$$

$$q_{t_2}^- = (a_1)^2 \frac{T_1 b_1 b_2 - T_2 a_1 a_2}{a_1^2 b_1 b_2 - b_1^2 a_1 a_2},$$

where $T_1 = Q_{\mu\mu} - a_0(Q_{o\mu} + Q_{\mu o}) + a_0^2 Q_{oo}$ and $T_2 = Q_{\nu\nu} - b_0(Q_{o\nu} + Q_{\nu o}) + b_0^2 Q_{oo}$.

The lower bound of q_{sum} is

$$q_{sum}^- = q_{t_1}^- + q_{t_2}^-. \quad (12)$$

B. Estimation of average intensity

In this subsection, we briefly introduce the simple tomography technique proposed by Ref.[24]. Based on this work, we propose a large random intensity fluctuation model in finite-key size regime.

As illustrated in Fig.4, Alice (Bob) should firstly produce a WCP with intensity $2x$ when she(he) actually wants x . Before sending the WCP to Charlie, she (he) splits it by a 50:50 BS. One of the pulse is sent to Charlie and the other one is measured by a local low dark-count SPD whose detection efficiency is η . After sending N_x x -intensity WCPs, the local detector's count number is n_x where the dark count is ignored since it's orders of magnitude lower than light count. Because of the random fluctuations, whenever Alice (Bob) wants to modulate intensity x , she (he) actually modulates $x_i = (1 + \delta_i)\bar{x}$, where \bar{x} is the average intensity and the instantaneous fluctuation δ_i is an unknown value. Mathematically, the click rate h_x is:

$$h_x = \sum_{i=0}^{N_x} (1 - e^{-\eta x_i}) / N_x. \quad (13)$$

As proof in Ref.[24], the upper and lower bound of \bar{x} is:

$$\begin{aligned}\bar{x} &\leq x_+ = \frac{1 - \sqrt{1 - 2h_x(1 + \zeta)}}{\eta(1 + \zeta)}, \\ \bar{x} &\geq x_- = h_x/\eta + h_x^2/2\eta - \eta^2 x_+^3/3!,\end{aligned}\tag{14}$$

where $\zeta = \sum \delta_i^2/N_x \leq (\text{Max}\{|\delta_i|\})^2$.

However, this conclusion in Ref.[24] can't be used in non-asymptotic situations directly. Here we apply large deviation theory to make the method met practice.

Noting that the distribution of intensity fluctuation is not independent identically distributed in most cases, we choose Azuma's inequality[41-43] rather than Chernoff bound to estimate the confidence interval of h_x . When the observed count number is \hat{n} , The upper and lower bound of h_x is:

$$\begin{aligned}h_x &\leq h_x^+ = (\hat{n} + \sqrt{2\hat{n}\ln\frac{1}{\epsilon_h}})/N_x, \\ h_x &\geq h_x^- = (\hat{n} - \sqrt{2\hat{n}\ln\frac{1}{\epsilon_h}})/N_x,\end{aligned}\tag{15}$$

where the ϵ_h is secure parameter of estimation. Then the bound of the average intensity is corrected as

$$\begin{aligned}\bar{x} &\leq x_+ = \frac{1 - \sqrt{1 - 2h_x^+(1 + \zeta)}}{\eta(1 + \zeta)}, \\ \bar{x} &\geq x_- = h_x^-/\eta + (h_x^-)^2/2\eta - \eta^2 x_+^3/3!.\end{aligned}\tag{16}$$

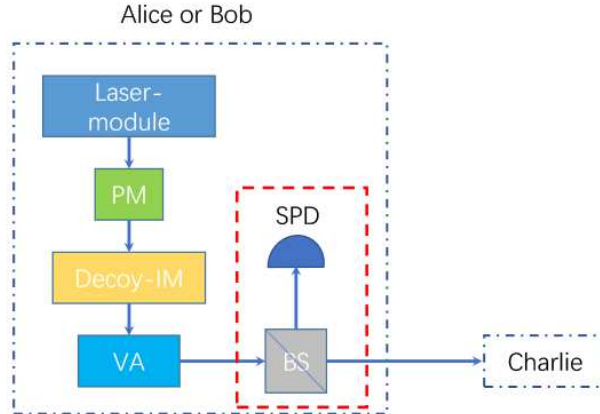


FIG. 4. The main structure of simple tomography technique is showed in the red dash line box. Alice (Bob) does all operations as usual except attenuate intensity to $2x$ when she (he) actually wants x , then she (he) splits it by a 50:50 BS. One of the pulse is sent to Charlie and the other is measured by a local low dark-count SPD. By observing the count rate of the local SPD, Alice (Bob) can estimate the bound of average intensity. PM denotes phase modulator, decoy-IM denotes intensity modulator. VA denotes variable attenuator. BS denotes 50:50 beam splitter and SPD denotes single photon detector.

C. Model of NPP-TFQKD with both intensity fluctuation and finite-key size effect

In this subsection, we will propose our countermeasure model. Firstly, we should define some symbols. Let's take the first decoy state(intensity is μ) as an example. When we want sent μ -intensity weak coherent pulse, we actually prepare $\mu_i = \bar{\mu}(1+\delta_i)$ since the intensity fluctuation. The intensity range is $\mu^\pm = \bar{\mu}(1+\delta^\pm)$ where $\delta^+ = \text{Max}\{\delta_i\}$ and $\delta^- = \text{Min}\{\delta_i\}$.

With definitions above, the density matrix of the source with fluctuation can be describe by:

$$\rho'_\mu = \sum_{i=1}^{N_\mu} \sum_{n=0}^{\infty} e^{-\mu_i} \frac{\mu_i^n}{n!} |n\rangle\langle n|/N_\mu, \quad (17)$$

and the a_n is re-written as:

$$a_n = \frac{1}{N_\mu} \sum_{i=1}^{N_\mu} e^{-\mu_i} \frac{\mu_i^n}{n!} = a_n = \frac{\bar{\mu}^n e^{-\bar{\mu}}}{n! N_\mu} \sum_{i=1}^{N_\mu} e^{-\delta_i \bar{\mu}} (1 + \delta_i)^n. \quad (18)$$

By applying taylor expansion to Eq.(18), we get:

$$\begin{aligned} a_n &= \frac{\bar{\mu}^n e^{-\bar{\mu}}}{n! N_\mu} \sum_{i=1}^{N_\mu} \left(1 - \delta_i \bar{\mu} + \frac{(\delta_i \bar{\mu})^2}{2!} - \dots\right) (1 + C_n^1 \delta_i + C_n^2 (\delta_i)^2 + \dots) \\ &= \frac{\bar{\mu}^n e^{-\bar{\mu}}}{n! N_\mu} \left[1 + \sum_{i=1}^{N_\mu} (n - \bar{\mu}) \delta_i + o(\delta_i)\right]. \end{aligned} \quad (19)$$

Noting an important fact that $\sum_{i=1}^{N_\mu} \delta_i = 0$, we find the first order item of δ is not exist in Eq.(19). i.e, the Eq.(19) can be re-written as:

$$a_n = \frac{\bar{\mu}^n e^{-\bar{\mu}}}{n! N_\mu} \left[\sum_{i=1}^{N_\mu} e^{-\delta_i \bar{\mu}} (1 + \delta_i)^n - \sum_{i=1}^{N_\mu} (n - \bar{\mu}) \delta_i \right]. \quad (20)$$

Define function $f_n(\delta) = e^{-\delta \bar{\mu}} (1 + \delta)^n - (n - \bar{\mu}) \delta$, $\delta \in [\delta_-, \delta_+]$. $f_n(\delta^u)$ and $f_n(\delta^l)$ are, respectively, maximum and minimum values which can be easily found by optimization algorithms in interval $[\delta_-, \delta_+]$. δ^u and δ^l are, respectively, maximum and minimum value points.

Noting that the function $g(\mu) = \frac{\mu^n e^{-\mu}}{n!}$ is monotonically increasing function when $n \geq 1$ and $\delta \in [-1, 1]$, when $n \geq 0$, we can obtain a tight bound of a_n as

$$\begin{aligned} a_n &\leq a_n^+ = \frac{(\mu^+)^n e^{-\mu^+}}{n!} f(\delta^u), \\ a_n &\geq a_n^- = \frac{(\mu^-)^n e^{-\mu^-}}{n!} f(\delta^l). \end{aligned} \quad (21)$$

Espacially, when $n = 0$,

$$a_0 \geq a_0^- = e^{-\mu^+}; \quad a_0 \leq a_0^+ = e^{-\mu^-}. \quad (22)$$

However, without introduction of average intensity, when $n \geq 1$:

$$a_n \geq a_n^- = \frac{e^{-\mu^-} (\mu^-)^n}{n!}, \quad a_n \geq a_n^+ = \frac{e^{-\mu^+} (\mu^+)^n}{n!}. \quad (23)$$

and when $n = 0$:

$$a_0 \geq a_0^- = e^{-\mu^+}, \quad a_0 \leq a_0^+ = e^{-\mu^-}. \quad (24)$$

The difference between introducing average intensity or not is showed in Fig.5, it indicates that the introduction of average intensity can significantly tighten the bound.

By substituting Eq.(3),(21) and (22) into our analytical formula, we can obtain bounds of q_{nm} in uncertain intensity and finite-key size regime.

Upper bound of q_{00} :

$$q_{00} = (a_0^+)^2 Q_{oo};$$

Upper bound of q_{10} and q_{01} :

We take q_{10}^+ as example, the q_{01}^+ is similar.

$$q_{10}^+ = a_0^+ a_1^+ \frac{K_2^+ (c_2^+ a_3^+ - c_3^- a_2^-) - K_1^- (b_3^+ c_2^+ - b_2^- c_3^-) - K_3^- (a_3^+ b_2^+ - a_2^- b_3^-)}{b_2^- (c_1^- a_3^- - a_1^+ c_3^+) - b_1^+ (c_2^- a_3^- - c_3^+ a_2^+) + b_3^- (a_2^- c_1^- - a_1^+ c_2^+)}, \quad (25)$$

where $K_1^- = Q_{\mu o}^- - a_0^+ Q_{oo}^+$, $K_2^+ = Q_{\nu o}^+ - b_0^- Q_{oo}^-$ and $K_3^- = Q_{\omega o}^- - c_0^+ Q_{oo}^+$.

Upper bound of q_{20} and q_{02} :

We take q_{20}^+ as example.

$$q_{20}^+ = a_0^+ a_2^+ \frac{H_1^+ c_1^+ - L_3^- a_1^-}{a_2^- c_1^- - a_1^+ c_2^+}, \quad (26)$$

where $H_1^+ = Q_{\mu o}^+ - a_0^- Q_{oo}^-$, $L_3^- = Q_{\omega o}^- - c_0^+ Q_{oo}^+ - (\sum_{n=3}^{\infty} c_n^+)$.

Upper bound of q_{11} :

$$q_{11}^+ = Q_{\mu\mu}^+ - a_0^- (Q_{\mu o}^- + Q_{o\mu}^-) + a_0^+ 2Q_{oo}^+. \quad (27)$$

Lower bound of q_{sum} :

$$\begin{aligned} q_{sum}^- &= q_{t1}^- + q_{t2}^-, \\ q_{t1}^- &= a_0^- [Q_{o\mu}^- + Q_{\mu o}^- - 2 \sum_{n=3}^{\infty} a_n^- - a_0^+ Q_{oo}^+], \\ q_{t2}^- &= \frac{T_2^- a_1^- a_2^- - T_1^+ b_1^+ b_2^+}{(a_1^+ b_1^+) (a_2^+ b_1^+ - a_1^- b_2^-)}, \end{aligned} \quad (28)$$

where $T_1^+ = Q_{\mu\mu}^+ - a_0^- (Q_{o\mu}^- + Q_{\mu o}^- - a_0^+ Q_{oo}^+)$ and $T_2^- = Q_{\nu\nu}^- - b_0^+ (Q_{o\nu}^+ + Q_{\nu o}^+ - b_0^- Q_{oo}^-)$.

The simulation of NPP-TFQKD with both large random intensity fluctuation and finite-key size effect is shown in Fig.6. We fix pulse number, dark-count rate, detection efficiency, misalignment, total secure parameter ϵ_{coh} and secure parameter of Azuma's inequality in Eq.(15) ϵ_h to 10^{14} , 10^{-10} , 14.5%, 1.5%, 10^{-10} and 10^{-10} respectively. To emphasize the countermeasure of intensity fluctuation, we simulate the SKR as a function of distance for different intensity fluctuation range and optimize SKR by PSO algorithm as introduced in Sec.III. The simulation result in Fig.6 indicates that by applying our countermeasure model, the large random intensity fluctuation has very limited influence on the performance of NPP-TFQKD.

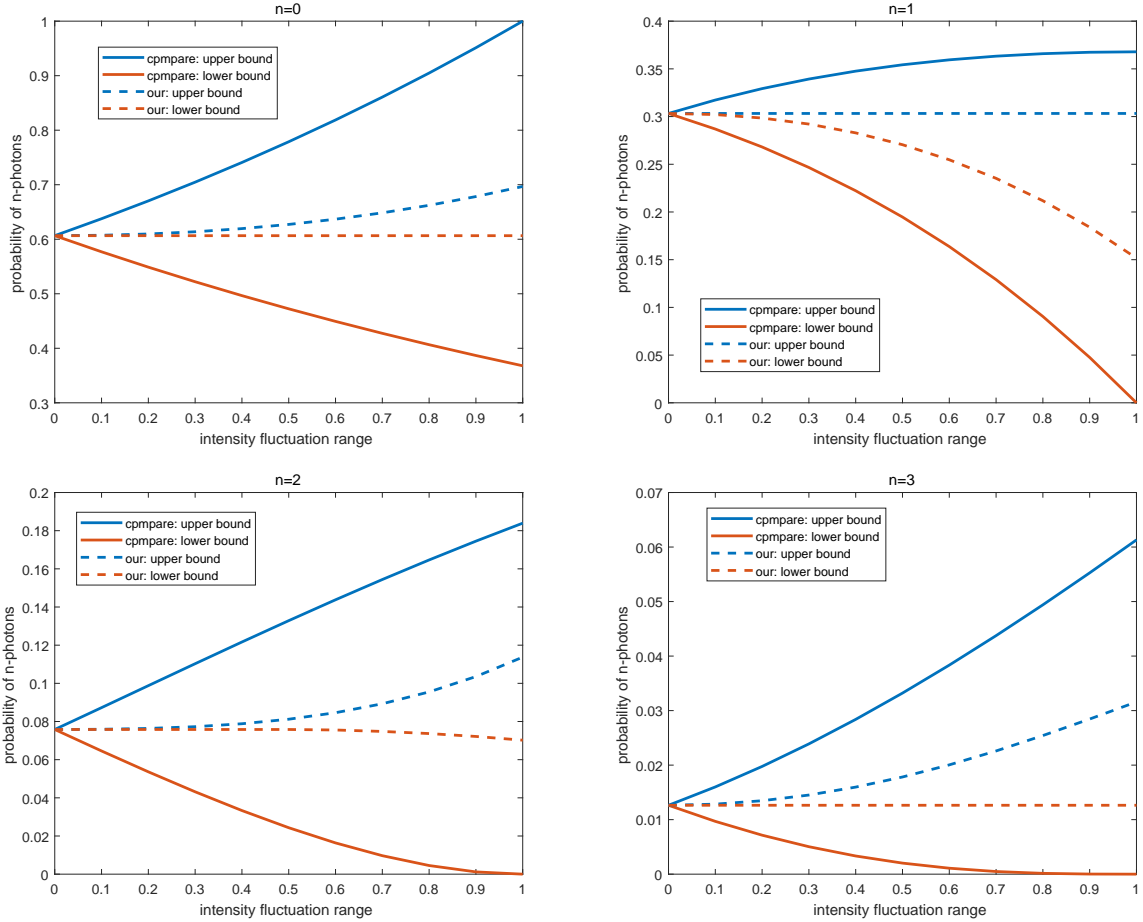


FIG. 5. We compare the upper and lower bound of a_n with two methods. The intensity is fixed at 0.5 and $n = 0, 1, 2, 3$ in different figures. In these figures, the blue and red lines denote the upper bound and lower bound respectively. The solid lines denote the model only considering fluctuation range and dash lines are our method which introducing the average intensity. It's obvious that our method estimates the bound much tighter.

V. CONCLUSION

In this article, we have discussed some practical issues of NPP-TFQKD based on Ref.[12]. We firstly analyzed the issue of finite-key size effect and solve this problem by applying post-selection technique for quantum channels[31] and using Chernoff Bound to estimate statistic fluctuations of observed values. The simulation shows that NPP-TFQKD works well in non-asymptotic situations.

Another contribution of this work is we propose a countermeasure of intensity fluctuation. We introduce an analytical formula of decoy state method to meet the needs of our fluctuation model. Then we propose our intensity fluctuation model to deal with large random intensity fluctuation problem in the source side. Our model is practical since it doesn't need any extra information except average intensity and fluctuation range. Our simulation results suggest that by applying our method, the non-asymptotic SKR can still break the linear bound even if the large random intensity fluctuation is taken into account.

This work has been supported by the National Key Research and Development Program of China (Grant No. 2016YFA0302600), the National Natural Science Foundation of China (Grant Nos. 61822115, 61775207, 61702469, 61771439, 61622506, 61627820, 61575183), National Cryptography Development Fund (Grant No. MMJJ20170120) and Anhui Initiative in Quantum Information Technologies.

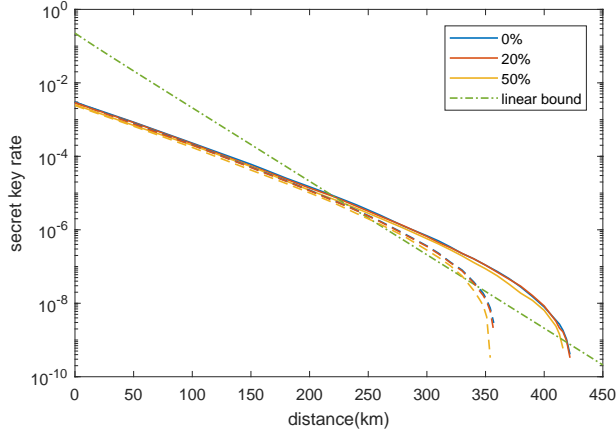


FIG. 6. Asymptotic secret key rate in logarithmic scale as a function of distance between Alice and Bob for different fluctuations and pulses number ($\delta^\pm = \pm 0\%$: blue, $\delta^\pm = \pm 20\%$: red, $\delta^\pm = \pm 50\%$: yellow. $N = 10^{14}$: solid lines, $N = 10^{13}$: dash lines). The green dot-dash line denotes linear bound.

APPENDIX: PROOF OF ANALYTICAL FORMULA

Firstly, we should introduce an important conclusion[29, 30]. $|\mu\rangle$ and $|\nu\rangle$ are coherent states, intensity μ is larger than ν . When $m > n$, there is:

$$\frac{p_m^\mu}{p_m^\nu} \geq \frac{p_n^\mu}{p_n^\nu} \quad (\mu \geq \nu ; m \geq n). \quad (29)$$

Upper bound of q_{00} :

The $Y_{00} = Q_{oo}$ since o is vacuum state. Thus:

$$q_{00} = a_0^2 Y_{00} = a_0^2 Q_{oo}. \quad (30)$$

Upper bound of q_{01} and q_{10} :

We take q_{01}^+ as an example and the proof of q_{10}^+ is similar. Define $K_1 = Q_{o\mu} - a_0 Q_{oo}$, $K_2 = Q_{o\mu} - b_0 Q_{oo}$, $K_3 = Q_{o\mu} - c_0 Q_{oo}$. Noting that $Q_{ox} - p_0^x Q_{oo} = p_1^x Y_{01} + p_2^x Y_{02} + p_3^x Y_{03} + \dots$, We get an equation set:

$$\begin{cases} K_1 = a_1 Y_{01} + a_2 Y_{02} + a_3 Y_{03} + \dots \\ K_2 = b_1 Y_{01} + b_2 Y_{02} + b_3 Y_{03} + \dots \\ K_3 = c_1 Y_{01} + c_2 Y_{02} + c_3 Y_{03} + \dots \end{cases} \quad (31)$$

By applying conclusion(29) and defining $\tau = \sum_{k=3}^{\infty} b_k Y_{0k}$, we can derive inequalities:

$$\begin{cases} K_1 b_3 / a_3 > a_1 b_3 Y_{01} / a_3 + a_2 b_3 Y_{02} / a_3 + \tau \\ K_2 = b_1 Y_{01} + b_2 Y_{02} + \tau \\ K_3 b_3 / c_3 < c_1 b_3 Y_{01} / c_3 + c_2 b_3 Y_{02} / c_3 + \tau \end{cases} \quad (32)$$

By solving Eq.(32), we obtain:

$$Y_{01} \leq Y_{01}^+ = \frac{K_2(c_2a_3 - c_3a_2) + K_1(b_2c_3 - b_3c_2) + K_3(a_2b_3 - a_3b_2)}{b_2(a_1c_3 - c_1a_3) + b_1(c_2a_3 - c_3a_2) + b_3(a_2c_1 - a_1c_2)}. \quad (33)$$

The upper bound of q_{01} is:

$$q_{01}^+ = a_0a_1Y_{01}^+. \quad (34)$$

Upper bound of q_{02} and q_{20} :

We take q_{02}^+ as an example. According to Eq.(7), we have:

$$\begin{aligned} Q_{o\mu} &\geq a_0Y_{00} + a_1Y_{01} + a_2Y_{02}; \\ Q_{ow} &\leq c_0Y_{00} + c_1Y_{01} + c_2Y_{02} + (c_3 + c_4 + c_5 + \dots). \end{aligned} \quad (35)$$

Noting that $Q_{oo} = Y_{00}$ and defining $H_1 = Q_{o\mu} - a_0Q_{oo}$ and $L_3 = Q_{ow} - c_0Q_{oo} - (c_3 + c_4 + c_5 + \dots)$, we obtain:

$$\begin{cases} H_1 > Y_{01}a_1 + Y_{02}a_2 \\ L_3 < Y_{01}c_1 + Y_{02}c_2 \end{cases} \quad (36)$$

By solving Eq.(36), we obtain:

$$Y_{02} < Y_{02}^+ = \frac{H_1c_1 - L_3a_1}{a_2c_1 - a_1c_2}. \quad (37)$$

The upper bound of q_{02} is:

$$q_{02}^+ = a_0a_2Y_{02}^+. \quad (38)$$

Upper bound of q_{11} :

It's easily to calculate \bar{q}_{11} by using $Q_{\mu\mu}$, $Q_{\mu o}$, $Q_{o\mu}$ and Q_{oo} :

$$q_{11} < \sum_{n=1, m=1}^{\infty} a_n a_m Y_{nm} = Q_{\mu\mu} - a_0Q_{\mu o} - a_0Q_{o\mu} + (a_0)^2Q_{oo}. \quad (39)$$

Thus the upper bound of q_{11} is:

$$q_{11}^+ = Q_{\mu\mu} - a_0Q_{\mu o} - a_0Q_{o\mu} + (a_0)^2Q_{oo}. \quad (40)$$

Lower bound of $q_{00} + q_{01} + q_{10} + q_{02} + q_{20} + q_{11}$: Define $q_{sum} = \sum_{n=0}^2 \sum_{m=0}^{2-m} q_{nm}$, $q_{t_1} = q_{00} + q_{01} + q_{10} + q_{02} + q_{20}$ and $q_{t_2} = q_{11}$. Obviously there is $q_{sum} = q_{t_1} + q_{t_2}$.

Firstly, we estimate the lower bound of q_{t_1} . It's obviously that:

$$q_{t_1} > q_{t_1}^+ = a_0[Q_{o\mu} + Q_{\mu o} - 2(a_3 + a_4 + a_5 + \dots)] - (a_0)^2Q_{oo}. \quad (41)$$

Then we estimate the lower bound of q_{t_2} . Similar to the estimation of q_{01}^+ , by defining $T_1 = Q_{\mu\mu} - a_0(Q_{o\mu} + Q_{\mu o}) + (a_0)^2Q_{oo}$, $T_2 = Q_{\nu\nu} - a_0(Q_{o\nu} + Q_{\nu o}) + (a_0)^2Q_{oo}$ and $\tau' = \sum_{m=1}^{\infty} \sum_{n=1}^{\infty} b_m b_n Y_{m,n} - (b_1)^2 Y_{1,1}$, we obtain an equation set:

$$\begin{cases} \frac{T_1 b_1 b_2}{a_1 a_2} < \frac{a_1 b_1 b_2 Y_{1,1}}{a_2} + \tau' \\ T_2 = (b_1)^2 Y_{1,1} + \tau' \end{cases} \quad (42)$$

Solve the Eq.(42), we obtain:

$$Y_{11} \geq Y_{11}^- = \frac{T_1 b_1 b_2 - T_2 a_1 a_2}{a_1^2 b_1 b_2 - b_1^2 a_1 a_2}, \quad (43)$$

and the lower bound of q_{t_2} is:

$$q_{t_2}^- = a_1^2 Y_{11}^-. \quad (44)$$

Our target, i.e. the lower bound of q_{sum} is:

$$q_{sum}^- = q_{t_1}^- + q_{t_2}^-. \quad (45)$$

- [1] C. H. Bennett and G. Brassard, *Theor. Comput. Sci.* **560**, 7 (2014).
- [2] A. K. Ekert, *Physical review letters* **67**, 661 (1991).
- [3] D. Mayers, *Journal of the ACM (JACM)* **48**, 351 (2001).
- [4] H.-K. Lo and H. F. Chau, *science* **283**, 2050 (1999).
- [5] P. W. Shor and J. Preskill, *Physical review letters* **85**, 441 (2000).
- [6] M. Takeoka, S. Guha, and M. M. Wilde, *Nat. Commun* **5**, 5235 (2014).
- [7] S. Pirandola, R. Laurenza, C. Ottaviani, and L. Banchi, *Nat. Commun.* **8**, 15043 (2017).
- [8] M. Lucamarini, Z. Yuan, J. Dynes, and A. Shields, *Nature* **557**, 400 (2018).
- [9] K. Tamaki, H.-K. Lo, W. Wang, and M. Lucamarini, arXiv preprint arXiv:1805.05511 (2018).
- [10] X. Ma, P. Zeng, and H. Zhou, arXiv preprint arXiv:1805.05538 (2018).
- [11] X.-B. Wang, Z.-W. Yu, and X.-L. Hu, *Physical Review A* **98**, 062323 (2018).
- [12] C. Cui, Z.-Q. Yin, R. Wang, W. Chen, S. Wang, G.-C. Guo, and Z.-F. Han, *Physical Review Applied* **11**, 034053 (2019).
- [13] M. Curty, K. Azuma, and H.-K. Lo, arXiv preprint arXiv:1807.07667 (2018).
- [14] J. Lin and N. Lütkenhaus, *Physical Review A* **98**, 042332 (2018).
- [15] M. Minder, M. Pittaluga, G. Roberts, M. Lucamarini, J. Dynes, Z. Yuan, and A. Shields, *Nature Photonics* p. 1 (2019).
- [16] S. Wang, D.-Y. He, Z.-Q. Yin, F.-Y. Lu, C.-H. Cui, W. Chen, Z. Zhou, G.-C. Guo, and Z.-F. Han, arXiv preprint arXiv:1902.06884 (2019).
- [17] Y. Liu, Z.-W. Yu, W. Zhang, J.-Y. Guan, J.-P. Chen, C. Zhang, X.-L. Hu, H. Li, T.-Y. Chen, L. You, et al., arXiv preprint arXiv:1902.06268 (2019).
- [18] X. Zhong, J. Hu, M. Curty, L. Qian, and H.-K. Lo, arXiv preprint arXiv:1902.10209 (2019).
- [19] H.-K. Lo, M. Curty, and B. Qi, *Physical review letters* **108**, 130503 (2012).
- [20] C. Wang, X.-T. Song, Z.-Q. Yin, S. Wang, W. Chen, C.-M. Zhang, G.-C. Guo, and Z.-F. Han, *Physical review letters* **115**, 160502 (2015).
- [21] Y. Liu, T.-Y. Chen, L.-J. Wang, H. Liang, G.-L. Shentu, J. Wang, K. Cui, H.-L. Yin, N.-L. Liu, L. Li, et al., *Physical review letters* **111**, 130502 (2013).
- [22] X. Ma and M. Razavi, *Physical Review A* **86**, 062319 (2012).
- [23] X.-B. Wang, L. Yang, C.-Z. Peng, and J.-W. Pan, *New Journal of Physics* **11**, 075006 (2009).
- [24] X.-B. Wang, *Physical Review A* **75**, 052301 (2007).
- [25] X.-Y. Zhou, C.-M. Zhang, and Q. Wang, *JOSA B* **34**, 1518 (2017).
- [26] H.-K. Lo, X. Ma, and K. Chen, *Physical review letters* **94**, 230504 (2005).
- [27] X.-B. Wang, *Physical Review A* **72**, 012322 (2005).
- [28] X.-B. Wang, *Physical review letters* **94**, 230503 (2005).
- [29] X.-B. Wang, *Physical Review A* **87**, 012320 (2013).

- [30] Z.-W. Yu, Y.-H. Zhou, and X.-B. Wang, *Physical Review A* **91**, 032318 (2015).
- [31] M. Christandl, R. König, and R. Renner, *Physical review letters* **102**, 020504 (2009).
- [32] L. Sheridan, T. P. Le, and V. Scarani, *New Journal of Physics* **12**, 123019 (2010).
- [33] X. Ma, C.-H. F. Fung, and M. Razavi, *Physical Review A* **86**, 052305 (2012).
- [34] M. Curty, F. Xu, W. Cui, C. C. W. Lim, K. Tamaki, and H.-K. Lo, *Nature communications* **5**, 3732 (2014).
- [35] J. Müller-Quade and R. Renner, *New Journal of Physics* **11**, 085006 (2009).
- [36] C. Wang, Z.-Q. Yin, S. Wang, W. Chen, G.-C. Guo, and Z.-F. Han, *Optica* **4**, 1016 (2017).
- [37] Y.-L. Tang, H.-L. Yin, S.-J. Chen, Y. Liu, W.-J. Zhang, X. Jiang, L. Zhang, J. Wang, L.-X. You, J.-Y. Guan, et al., *Physical review letters* **113**, 190501 (2014).
- [38] F.-Y. Lu, Z.-Q. Yin, and C. Wang, *JOSA B* **36**, 92 (2019).
- [39] W. Wang and H.-K. Lo, arXiv preprint arXiv:1812.07724 (2018).
- [40] J. Kennedy, *Encyclopedia of machine learning* pp. 760–766 (2010).
- [41] Z. Q. Yin, H. W. Li, W. Chen, Z. F. Han, and G. C. Guo, *Phys. Rev. A* **82**, 042335 (2010).
- [42] J. C. Boileau, K. Tamaki, J. Batuwantudawe, R. Laflamme, and J. M. Renes, *Phys. Rev. Lett.* **94**, 040503 (2005).
- [43] K. Azuma, *Tohoku Math. J.* **19**, 357 (1967).